J|A|C|S
ARTICLES
Published on Web 04/21/2007

The Solvent Cage Effect: Is There a Spin Barrier to Recombination of Transition Metal Radicals?

John D. Harris, Alan B. Oelkers, and David R. Tyler*

Contribution from the Department of Chemistry, University of Oregon, Eugene, Oregon 97403

Received January 8, 2007; E-mail: dtyler@uoregon.edu

Abstract: This investigation explored whether there is a spin barrier to recombination of first- and second-row transition metal-centered radicals in a radical cage pair. To answer this question, the recombination efficiencies of photochemically generated radical cage pairs (denoted as F_{cP}) were measured in the presence and absence of an external heavy atom probe. Two methods were employed for measuring the cage effect. The first method was femtosecond pump−probe transient absorption spectroscopy, which directly measured F_{cP} from reaction kinetics, and the second method (referred to herein as the "steady-state" method) obtained F_{cP} from quantum yields for the radical trapping reaction with CCl_4 as a function of solvent viscosity. Both methods generated radical cage pairs by photolysis ($\lambda = 515$ nm for the pump probe method and $\lambda = 546$ nm for the steady-state method) of $Cp'_2Mo_2(CO)_6$ ($Cp' = \eta^5$-$C_5H_4CH_3$). In addition, radical cage pairs generated from $Cp'_2Fe_2(CO)_4$ and $Cp^*_2TiCl_2$ ($Cp^* = \eta^5$-$C_5(CH_3)_5$) were studied by the steady-state method. The pump−probe method used *p*-dichlorobenzene as the heavy atom perturber, whereas the steady-state method used iodobenzene. For both methods and for all the radical caged pairs investigated, there were no observable heavy atom effects, from which it is concluded there is no spin barrier to recombination.

Introduction

The concept of the "cage effect" was introduced by Franck and Rabinowitch in 1934 to explain why the quantum yield of I_2 photodissociation was lower in solution than in the gas phase.[1−3] It was proposed that, following bond photolysis, the solvent temporarily encapsulates the reactive I· atoms in a "solvent cage," causing them to remain as colliding neighbors for a short time before they either recombine or diffuse apart. This concept is illustrated for a general photolysis reaction in Scheme 1. In the years since the initial description by Franck and Rabinowitch, cage effects have been shown to have a major impact on chemical reactivity in solution.[4−67]

For quantitative discussions, the "cage recombination efficiency" (denoted as F_c and sometimes colloquially called the "cage effect") is defined as the ratio of the rate constant for recombination to the sum of all possible cage processes. For the reaction in Scheme 1, $F_c = k_c/(k_c + k_d)$.[52] F_c for a photochemically formed radical cage pair does not necessarily equal F_c for the same cage pair formed by thermolysis or by diffusional collision of two free radicals.[53,54] To differentiate these cases, the cage efficiency of photochemically generated radical cage pairs will be denoted F_{cP} in this paper and the associated rate constants k_{cP} and k_{dP}.

(1) Rabinowitch, E.; Wood, W. C. *Trans. Faraday Soc.* **1936**, *32*, 1381−1387.
(2) Franck, J.; Rabinowitsch, E. *Trans. Faraday Soc.* **1934**, *30*, 120−131.
(3) Rabinowitch, E. *Trans. Faraday Soc.* **1937**, *33*, 1225−1233.
(4) Lorand, J. P. *Prog. Inorg. Chem.* **1972**, *17*, 207−325.
(5) Rice, S. A. *Comprehensive Chemical Kinetics*; Elsevier: Amsterdam, Netherlands, 1985; Vol. 25.
(6) Koenig, T. W.; Hay, B. P.; Finke, R. G. *Polyhedron* **1988**, *7*, 1499−1516.
(7) Cage effects are necessary to explain a host of kinetic observations and fundamental reaction phenomena. Examples of important reactions where cage effects are necessary to explain the kinetics include radical polymerization reactions,[8−12] the reactions of coenzyme B_{12} and its model complexes,[13−17] the reactions of hemes with O_2,[18] the reactions of photosynthetic model complexes, and numerous electron transfer reactions.[19,20] The literature is replete with new observations of the cage effect and its impact on reactivity. For example, the repercussions of cage effects in confined media such as micelles and zeolites,[21−25] biochemical toxicity,[26] supercritical fluids,[27] polymer degradation reactions,[28−31] chemiluminescence,[32−34] bond cleavage energetics,[35] and in metal complex photochemistry[36] are areas of current study. Furthermore, cage effects are necessary to explain some of the most fundamental phenomena in physical- and physical organic-chemistry, including magnetic isotope[37,38] and CIDNP[39,40] effects, rate-viscosity correlations,[41] variations in products and yields as a function of medium,[42] variations in quantum yields as a function of medium,[43] and stereochemical control.[44,45] In addition, analogues of solvent-phase cage effects have now been observed in reactions taking place on surfaces[46,47] and in gas-phase clusters.[48−51]
(8) Bosch, P.; Mateo, J. L.; Serrano, J. *J. Photochem. Photobiol. A* **1997**, *103*, 177−184.
(9) Wolff, E.-H. P.; Bos, A. N. R. *Ind. Eng. Chem. Res.* **1997**, *36*, 1163−1170.
(10) Frounchi, M.; Farhadi, F.; Mohammadi, R. P. *Sci. Iran.* **2002**, *9*, 86−92.
(11) Capek, I. *Adv. Colloid Interface Sci.* **2001**, *91*, 295−334.
(12) De Kock, J. B. L.; Van Herk, A. M.; German, A. L. *J. Macromol. Sci. Poly. Rev.* **2001**, *C41*, 199−252.
(13) Cole, A. G.; Yoder, L. M.; Shiang, J. J.; Anderson, N. A.; Walker, L. A., II; Banaszak Holl, M. M.; Sension, R. J. *J. Am. Chem. Soc.* **2002**, *124*, 434−441.
(14) Yoder, L. M.; Cole, A. G.; Walker, L. A., II; Sension, R. J. *J. Phys. Chem. B* **2001**, *105*, 12180−12188.
(15) Shiang, J. J.; Walker, L. A., II; Anderson, N. A.; Cole, A. G.; Sension, R. J. *J. Phys. Chem. B* **1999**, *103*, 10532−10539.
(16) Walker, L. A., II; Shiang, J. J.; Anderson, N. A.; Pullen, S. H.; Sension, R. J. *J. Am. Chem. Soc.* **1998**, *120*, 7286−7292.
(17) Natarajan, E.; Grissom, C. B. *Photochem. Photobiol.* **1996**, *64*, 286−295.
(18) Grogan, T. G.; Bag, N.; Traylor, T. G.; Magde, D. *J. Phys. Chem.* **1994**, *98*, 13791−13796.
(19) Van Dijk, H. K.; Van der Haar, J.; Stufkens, D. J.; Oskam, A. *Inorg. Chem.* **1989**, *28*, 75−81.
(20) Knoll, H.; De Lange, W. J. G.; Hennig, H.; Stufkens, D. J.; Oskam, A. *J. Organomet. Chem.* **1992**, *430*, 123−132.
(21) Flachenecker, G.; Behrens, P.; Knopp, G.; Schmitt, M.; Siebert, T.; Vierheilig, A.; Wirnsberger, G.; Materny, A. *J. Phys. Chem. A* **1999**, *103*, 3854−3863.
(22) Karprinidis, N. A.; Landis, M. S.; Turro, N. J. *Tetrahedron Lett.* **1997**, *38*, 2609−2612.

Scheme 1. Photolysis of a Generic Molecule in Solution to Yield a Radical Cage Pair[a]

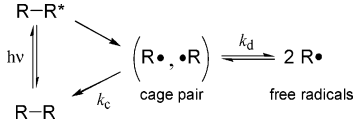

[a] Radicals in the solvent cage can either diffuse apart to yield free radicals or recombine to reform the parent molecule. The rate constants k_c and k_d are for radical−radical recombination and for radical diffusion out of the cage, respectively.

Scheme 2. Photolysis of a Generic Dimer to Form Singlet and Triplet Radical Cage Pairs[a]

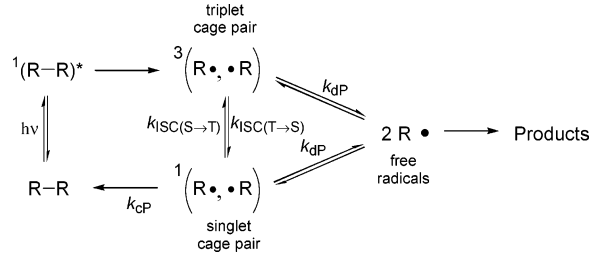

[a] Triplet cage pair must intersystem cross (with rate constant $k_{ISC(T→S)}$) to the singlet state before recombination can occur.

A more complete reaction scheme showing the spin state of the cage pair radicals formed in a typical photochemical reaction is shown in Scheme 2. A key point is that, classically, only singlet-state radical cage pairs can recombine; triplet state cage pairs must first intersystem cross to the singlet state before recombination.[40,55,56] A spin barrier occurs when the rate of triplet to singlet intersystem crossing (ISC), $k_{ISC(T→S)}$, is slow compared to the rate of recombination, k_{cP}. Under such conditions, the rate of ISC affects the value of F_{cP}. For carbon-centered radicals, spin barriers are well-known and have been studied for their impact on both photophysical[57,58] and photochemical processes.[59−62]

A common method of studying spin barriers is to use a heavy atom as a probe. The rate of intersystem crossing, k_{ISC}, is approximately proportional to the square of the effective spin−orbit coupling constant, ζ_l, i.e., $k_{ISC} \propto \zeta_l^2$.[60] Because ζ_l (and thus k_{ISC}) increase with nuclear charge, Z, the phenomenon is called the heavy atom effect.[61,63] Although ζ_l increases as Z increases, shielding of the valence electrons by the core electrons keeps ζ_l from being solely dependent on Z so that a large Z does not directly correspond to a large ζ_l. For example, barium has $Z = 56$, but has $\zeta_l = 830$ cm^{-1}, while iodine has $Z = 53$, but has $\zeta_l = 5069$ cm^{-1}.[64,65] The general trend for ζ_l, and hence for k_{ISC}, is that it increases the farther down and to the right an element is in the periodic table.[63,65,66] Both internal and external heavy atom effects are well-documented.[58,59,63,67] For internal heavy atom effects, the perturbing heavy atom is covalently bonded to the photoactive species, whereas for external heavy atom effects, the perturbing atom is either a solute or the solvent itself.[68,69] The majority of the photophysical and photochemical studies of the heavy atom effect have focused on carbon-centered radicals, where Br or I are used as the perturbing heavy atoms. In these studies, the heavy atom effects on the spin-state of the excited molecules are either directly monitored using spectroscopic methods or they are monitored indirectly by measuring ratios of isomeric products, where the identity of the product is determined by the spin state of the excited precursor (see below).[57−62]

It is generally assumed that, for transition metal-centered radicals, there is no spin barrier to radical−radical combination because the transition metals act as heavy atoms. However, data in support of this assumption are limited. In fact, recent work suggests that spin barriers can play an important role in oxidation reactions, C−H bond activation reactions, and ligand-association reactions of coordinatively unsaturated transition metal com-

(23) Turro, N. J.; Lei, X.-G.; Li, W.; Liu, Z.; McDermott, A.; Ottaviani, M. F.; Abrams, L. *J. Am. Chem. Soc.* **2000**, *122*, 11649−11659.
(24) Abrams, L.; Corbin, D. R.; Turro, N. J. *Stud. Surf. Sci. Catal.* **1987**, *39*, 519−529.
(25) Sivaguru, J.; Natarajan, A.; Kaanumalle, L. S.; Shailaja, J.; Uppili, S.; Joy, A.; Ramamurthy, V. *Acc. Chem. Res.* **2003**, *36*, 509−521.
(26) Goldstein, S.; Czapski, G. *J. Am. Chem. Soc.* **1999**, *121*, 2444−2447.
(27) Tanko, J. M.; Suleman, N. K.; Fletcher, B. *J. Am. Chem. Soc.* **1996**, *118*, 11958−11959.
(28) Guillet, J. *Polymer Photophysics and Photochemistry: An Introduction to the Study of Photoprocesses in Macromolecules*; Cambridge University Press: New York, 1985.
(29) Guillet, J. *Adv. Photochem.* **1988**, *14*, 91−133.
(30) Shlyapnikov, Y. A.; Kiryushkin, S. G.; Marin, A. P. *Antioxidative Stabilization of Polymers*; Taylor and Francis: Bristol, PA, 1996.
(31) Allen, N. S. *Photochemistry* **2001**, *32*, 343−405.
(32) Adam, W.; Bronstein, I.; Trofimov, A. V.; Vasil'ev, R. F. *J. Am. Chem. Soc.* **1999**, *121*, 958−961.
(33) Lee, S. H.; Mendenhall, G. D. *J. Am. Chem. Soc.* **1988**, *110*, 4318−4323.
(34) Mendenhall, G. D.; Matisova-Rychla, L. *J. Photochem. Photobiol. A* **1994**, *83*, 21−27.
(35) Koenig, T.; Finke, R. G. *J. Am. Chem. Soc.* **1988**, *110*, 2657−2658.
(36) Farias de Lima, J.; Nakano, A. K.; Iha, N. Y. M. *Inorg. Chem.* **1999**, *38*, 403−405.
(37) Turro, N. J.; Kraeutler, B. *Acc. Chem. Res.* **1980**, *13*, 369−377.
(38) Lott, W. B.; Chagovetz, A. M.; Grissom, C. B. *J. Am. Chem. Soc.* **1995**, *117*, 12194−12201.
(39) Kaptein, R. *Advances in Free-Radical Chemistry (London)* **1975**, *5*, 319−380.
(40) Woodward, J. R. *Prog. React. Kinet. Mech.* **2002**, *27*, 165−207.
(41) Rembaum, A.; Szwarc, M. *J. Chem. Phys.* **1955**, *23*, 909−913.
(42) Tanner, D. D.; Oumar-Mahamat, H.; Meintzer, C. P.; Tsai, E. C.; Lu, T. T.; Yang, D. *J. Am. Chem. Soc.* **1991**, *113*, 5397−5402.
(43) Noyes, R. M. *Z. Elektrochem. Angew. Phys. Chem.* **1960**, *64*, 153−156.
(44) Maleczka, R. E., Jr.; Geng, F. *J. Am. Chem. Soc.* **1998**, *120*, 8551−8552.
(45) Tomooka, K.; Yamamoto, H.; Nakai, T. *Angew. Chem., Int. Ed.* **2000**, *39*, 4500−4502.
(46) Jenks, C. J.; Paul, A.; Smoliar, L. A.; Bent, B. E. *J. Phys. Chem.* **1994**, *98*, 572−578.
(47) Buchanan, A. C.; III; Britt, P. F.; Thomas, K. B. *Energy Fuels* **1998**, *12*, 649−659.
(48) Vorsa, V.; Nandi, S.; Campagnola, P. J.; Larsson, M.; Lineberger, W. C. *J. Chem. Phys.* **1997**, *106*, 1402−1410.
(49) Su, J. T.; Zewail, A. H. *J. Phys. Chem. A* **1998**, *102*, 4082−4099.
(50) Materny, A.; Lienau, C.; Zewail, A. H. *J. Phys. Chem.* **1996**, *100*, 18650−18665.
(51) Kanaev, A.; Museur, L.; Edery, F.; Laarmann, T.; Moller, T. *J. Chem. Phys.* **2002**, *117*, 9423−9429.
(52) In addition to recombination and diffusive separation, the chemical reactions of cage pairs can include disproportionation, isomerizations, fragmentations, electron transfer, in-cage trapping, etc. For the metal-radical cage pairs in this paper, the only chemical process is *kc*.
(53) Koenig, T.; Fischer, H. *Free Radicals* **1973**, *1*, 157−189.
(54) Koenig, T. W. *ACS Symp. Ser.* **1978**, *69*, 134−160.
(55) Turro, N. J. *Proc. Natl. Acad. Sci. U.S.A.* **1983**, *80*, 609−621.
(56) Ingold, K. U. In *Free Radicals*; Wiley: New York, 1973; Vol. 1, pp 37−112.
(57) Kasha, M. *J. Chem. Phys.* **1952**, *20*, 71−74.
(58) Chandra, A. K.; Turro, N. J.; Lyons, A. L., Jr.; Stone, P. *J. Am. Chem. Soc.* **1978**, *100*, 4964−4968.
(59) Inoue, H.; Sakurai, T.; Hoshi, T.; Okubo, J.; Ono, I. *Chem. Lett.* **1990**, 1059−1062.
(60) Kikuchi, K.; Hoshi, M.; Abe, E.; Kokubun, H. *J. Photochem. Photobiol. A* **1988**, *45*, 1−7.
(61) Koziar, J. C.; Cowan, D. O. *Acc. Chem. Res.* **1978**, *11*, 334−341.
(62) Kikuchi, K.; Hoshi, M.; Niwa, T.; Takahashi, Y.; Miyashi, T. *J. Phys. Chem.* **1991**, *95*, 38−42.
(63) Winter, G.; Steiner, U. *Ber. Buns-Ges.* **1980**, *84*, 1203−1214.
(64) Murov, S. L. C., I.; Hug, G. L. *Handbook of Photochemistry*, 2nd ed.; Marcel Dekker, Inc.: New York, 1993.
(65) Khudyakov, I. V.; Serebrennikov, Y. A.; Turro, N. J. *Chem. Rev.* **1993**, *93*, 537−570.
(66) Hess, B. A. *Ber. Buns-Ges.* **1997**, *101*, 1−10.
(67) Tero-Kubota, S.; Katsuki, A.; Kobori, Y. *J. Photochem. Photobiol. C. Photochem. Rev.* **2001**, *2*, 17−33.
(68) Berberan-Santos, M. N. *PhysChemComm [Electronic Publication]* **2000**, *3*, Article No 5.
(69) Cowan, D. O.; Koziar, J. C. *J. Am. Chem. Soc.* **1974**, *96*, 1229−1230.

Scheme 3. Photolysis of Diazoacetonitrile α-Methylmercuridiazoacetonitrile in *cis*-2-Butene

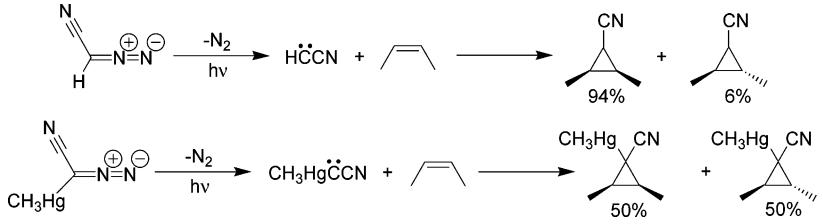

plexes.[70,71] Accordingly, to understand better the role of spin in the recombination of transition metal-centered radical cage pairs, we began an investigation of heavy atom effects in the recombination of cage pairs involving Fe-, Mo-, and Ti-centered radicals. In this paper, we report the results of our study.

It is noted that, although the presence of transition metals on the rate of radical−radical recombination has not been studied for transition metal-centered radicals, a limited number of prior studies have shown that transition metals can act as heavy atoms by affecting the rate of radical−radical recombination in carbon-centered radicals and by affecting the rate of ISC in excited states. For example, Skell et al. studied spin barriers in the photolysis of diazoacetonitrile and the impact of including an −HgR group in the molecule.[72] Upon photolysis, diazoacetonitrile loses N_2 to form a singlet carbene (Scheme 3). This singlet carbene can either react stereospecifically with an alkene to give the cis product or intersystem cross to the triplet state before reacting to form the trans product. When diazoacetonitrile is photolyzed in *cis*-2-butene, the cis-to-trans product ratio is 47:3. However, when a −HgR group is included in the diazoacetonitrile molecule, its presence increases k_{ISC}, and the cis-to-trans product ratio is 1:1 (Scheme 3).[72]

In other work, the presence of transition metals has been shown to impact the spin state of metalloporphyrins. Several researchers have shown that the addition of a cationic metal to a free-base porphyrin suppresses the intensity of fluorescence.[72−75] These results were interpreted as being caused by an internal heavy atom effect, which facilitates a mixing of states. Consistent with this interpretation, Azenha et al. measured $k_{ISC(S\rightarrow T)}$ for a series of metallotetrakisphenylporphyrins (MTPP) and found that $k_{ISC(S\rightarrow T)}$ increased as the ζ_l of the metal increased.[73]

Another area where there has been intense interest on spin-state effects is in incorporating transition metals into a polymer as a means to control and tune different properties of the polymer, e.g., the redox, optical, and electronic properties.[76,77] For example, Liu et al. examined a series of polyynes and model monomers containing either platinum(II), gold(I), or mercury-(II) with biphenyl spacers.[77] They found that incorporation of a transition metal into the polymer resulted in more efficient ISC as indicated by a larger rate constant for phosphorescence radiative decay (k_r). (For aromatic hydrocarbons, $k_r = 0.1-1$ s^{-1}, while for metallopolyyne polymers, $k_r = 7.8 \times 10^5$ to 2.1×10^6 s^{-1}.) In another study, Rogers et al. looked at the effects of Pt incorporation into polymeric butadiynes, shown below, where $n = 1-3$.[76]

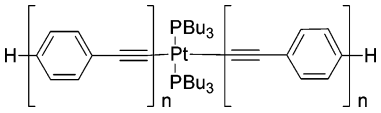

They found that the presence of Pt decreased the triplet state lifetime compared to the nonmetallated butadiynes and that the effect of Pt diminished as *n* increased.[76]

Experimental Section

Instrumentation and Reagents. All manipulations were carried out in the absence of water and atmospheric oxygen using standard glove box techniques. Due to the light-sensitive nature of the organometallic complexes, all samples were prepared in the darkroom and carefully protected from exposure to light. $Cp'_2Mo_2(CO)_6$ and $Cp'_2Fe_2(CO)_4$ were synthesized and purified as described in the literature.[78,79] $Cp^*_2TiCl_2$ (Strem Chemical Co., 99%), *p*-dichlorobenzene (Aldrich, 99%), and squalane (Aldrich, 99%) were obtained from their respective suppliers and used as received. Hexane (Fischer), carbon tetrachloride (Aldrich), iodobenzene (Aldrich), chlorobenzene (Aldrich), and benzene (Fischer) were purified according to standard literature techniques.[80]

A Nicolet Magna 500 FT-IR spectrometer with OMNIC software was used for all of the infrared spectra. A Hewlett-Packard 8453 UV−vis spectrophotometer was used for all of the electronic absorption spectra. A Varian Unity/Inova 300 spectrometer operating at a frequency of 299.95 Hz was used for ^{1}H NMR spectra.

F_{cp} Obtained from Quantum Yields as a Function of Viscosity. An Oriel Merlin radiometry system was used to monitor the photoreactions, which consists of: 1) an Oriel 200 W high-pressure mercury arc lamp, 2) an Oriel 100 mm^2, NIST calibrated silicon photodiode (model 70356) detector, 3), an Oriel Merlin radiometer control unit, 4), and an IBM personal computer. The concentration of caged radical precursors ($Cp'_2Mo_2(CO)_6$, $Cp'_2Fe_2(CO)_4$, or $Cp^*_2TiCl_2$) was chosen so that the resultant solution gave an absorbance between 0.8 and 1.5. All of the solutions contained 60% (v/v) of the hexane/squalane solvent system, 17.5% (v/v) carbon tetrachloride, used as the

(70) Harvey, J. N.; Poli, R.; Smith, K. M. *Coord. Chem. Rev.* **2003**, *238*−*239*, 347−361.
(71) Poli, R.; Harvey, J. N. *Chem. Soc. Rev.* **2003**, *32*, 1−8.
(72) Engelmann, F. M.; Mayer, I.; Araki, K.; Toma, H. E.; Baptista, M. S.; Maeda, H.; Osuka, A.; Furuta, H. *J. Photochem. Photobiol. A* **2004**, *163*, 403−411.
(73) Azenha, E. G.; Serra, A. C.; Pineiro, M.; Pereira, M. M.; De Melo, J. S.; Arnaut, L. G.; Formosinho, S. J.; Gonsalves, A. M. d. A. R. *Chem. Phys.* **2002**, *280*, 177−190.
(74) Valicsek, Z.; Horvath, O.; Stevenson, K. L. *Photochem. Photobiol. Sci.* **2004**, *3*, 669−673.
(75) Cheng, K. F.; Drain, C. M.; Grohmann, K. *Inorg. Chem.* **2003**, *42*, 2075−2083.
(76) Rogers, J. E.; Hall, B. C.; Hufnagle, D. C.; Slagle, J. E.; Ault, A. P.; McLean, D. G.; Fleitz, P. A.; Cooper, T. M. *J. Chem. Phys.* **2005**, *122*, 214708/1−214708/8.
(77) Liu, L.; Poon, S.-Y.; Wong, W.-Y. *J. Organomet. Chem.* **2005**, *690*, 5036−5048.
(78) King, R. B.; Stone, F. G. A. *Inorg. Syn.* **1963**, *7*, 99−115.
(79) Birdwhistell, R.; Hackett, P.; Manning, A. R. *J. Organomet. Chem.* **1978**, *157*, 239−241.
(80) Perrin, D. D.; Armarego, W. L. F. *Purification of Laboratory Chemicals*, 3rd ed.; Pergamon Press: New York, 1988.

radical trap, and 22.5% (v/v) of either the heavy atom probe (iodobenzene) or the control (chlorobenzene). (Before measuring F_{cp}, all solutions were tested for any unanticipated dark reactions between the caged radical precursors and the iodobenzene or the chlorobenzene.) A 2.5 mL aliquot of each solution was added to a gastight cuvette and each solution composition was then analyzed in five replicate samples. During the experiment, the solutions were maintained at a constant temperature of 23.0 ± 0.1 °C. The absolute viscosities of the samples were measured in triplicate using calibrated Cannon-Fenske viscometers. The temperature of both the viscometer and solutions were equilibrated in a water bath (23.0 ± 0.1 °C) for 10 min before each measurement.

Femtosecond Transient Absorption Spectroscopy. The full details of the femtosecond laser system and experimental design have been described.[81] Briefly, the master oscillator is a home-built, passively mode-locked Ti:Sapphire oscillator, pumped with a continuous wave (cw) frequency-doubled Nd:YVO_4 laser (Spectra-Physics Millenia). The femtosecond oscillator produces a train of *ca.* 100 fs femtosecond pulses at an 80 MHz repetition frequency and central wavelength of 800 nm. The oscillator output is directed into a stretched-chirped pulse regenerative amplifier (Spectra-Physics Spitfire). The regenerative amplifier is pumped by a Q-switched (1 kHz) frequency-doubled Nd:YLF laser source (Spectra-Physics Evolution). The amplifier produces a 1 kHz pulse train of 100 fs pulses with frequency centered at 800 nm, with total energy of 1 W (1 mJ/pulse). The amplifier output is split into probe and pump pulse trains using a thin dielectric beamsplitter. The pump pulse train with 515 nm wavelength is generated by optical parametric amplification (OPA) (Spectra-Physics). The probe pulse train is generated as the second harmonic of the 800 nm fundamental using a 0.5 mm type II β-barium borate (BBO) crystal. A paired-prism pulse compressor is used to eliminate second-order chirp in both pump and probe pulse trains in an effort to maintain the minimum time-bandwidth product at the sample interface. To collect isotropic data, the polarization of the pump pulse train is rotated to the magic angle (54.7°) w.r.t the probe pulse using a broadband $\lambda/2$ waveplate and a thin film polarizer. The probe pulse is temporally delayed by a mechanical translation stage (Aerotech ATS-2060). The differential absorption of the systems studied was obtained by modulating the pump repetition frequency to 500 Hz, or $^1/_2$ the probe repetition rate, using a mechanical chopper. The pump and probe pulses are focused to a diameter of 500 and 200 μm, respectively, at the flow cell interface, where the spot size measurement and the alignment of the pump and probe beams was achieved through the use of a set of precision-mounted pinhole apertures. The pump and probe pulse energies were approximately 8 and 0.5 μJ, respectively and the transient signal was found to be linear with pump power, indicating a one-photon process. Data was collected using a biased silicon photodiode (Thorlabs DET-210), sampled with a boxcar averager (SRS-SR250) and transferred to a computer through an A/D converter. Accurate synchronization is obtained by indexing the probe signal to the 500 Hz pump signal, collected with a separate photodiode and boxcar set.

Because the compounds are air sensitive, the flow cell system was designed to be anaerobic. The flow cell system consists of a stainless-steel reservoir, a magnetically driven inert-fluid mechanical pump, stainless-steel tubing, and a custom-built stainless-steel flow cell with 1 mm thick CaF_2 windows and a 500 μm path length. The flow cell system was leak-checked under vacuum, and all solutions were deoxygenated prior to loading in the reservoir. The integrity of the studied samples was confirmed after laser studies by UV−vis absorption measurements.

Photodimerization of Coumarin. Solutions containing 0.3 M coumarin in benzene, carbon tetrachloride, and benzene/2.0 M chlorobenzene were prepared using standard glove box techniques. Aliquots (2.5 mL) of each solution were syringed into a gastight cuvette and each solution was analyzed in triplicate. The solutions were simultaneously irradiated for 85 h in a carousel apparatus using a 200 W high-pressure mercury arc lamp fitted with an IR Corning UV filter (1−58) (long irradiation times were necessary due to the low quantum yield of dimerization for coumarin).[82] The product was attained by rotovaping off the solvent and subliming off any unreacted coumarin. The anti head-to-head dimer was characterized by ^{1}H NMR spectroscopy. (See the Supporting Information.)

Results and Discussion

General Strategy. If a spin barrier is present in the recombination of radical cage pairs, it will be most noticeable in systems containing lighter elements. For that reason, in this study radical cage pairs were investigated that contained (a) first-row transition metal-centered radicals, (b) second-row transition metal-centered radicals, and (c) a carbon-centered radical and a first-row transition metal radical. Specifically, radical cage pairs were generated by photolysis of $Cp'_2Mo_2(CO)_6$, $Cp'_2Fe_2(CO)_4$, and $Cp^*_2TiCl_2$ according to the reactions in eq 1−3. (The ζ_l values (cm^{-1}) for the relevant elements used in this study are as follows: Mo, 678; Fe, 431; Ti, 123; C, 32; I, 5069; Cl, 587; Br, 2460.)[64]

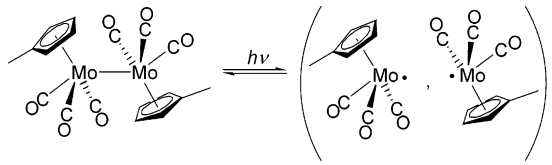

(1)

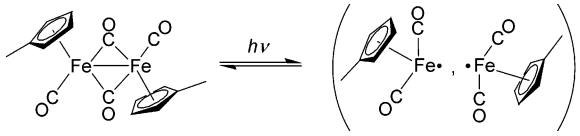

(2)

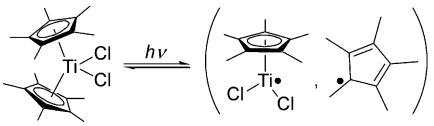

(3)

F_{cP} values for the radical cage pairs produced in these reactions were measured in the presence and absence of an external heavy atom probe: 2.0 M *p*-dichlorobenzene in the pump−probe experiments or 2.0 M iodobenzene in the steady-state experiments. Note that the steady-state method is extremely sensitive to solvent conditions, thus in the absence of 2.0 M iodobenzene, 2.0 M chlorobenzene was added as a replacement

(81) Oelkers, A. B.; Scatena, L.; Tyler, D. R. *J. Phys. Chem. A* **2007**, submitted for publication.

(82) Hoffman, R.; Wells, P.; Morrison, H. *J. Org. Chem.* **1971**, *36*, 102−108.

Scheme 4. Proposed Mechanism for the Dimerization or Dissociation of the Coumarin Dimer Triplet Biradical

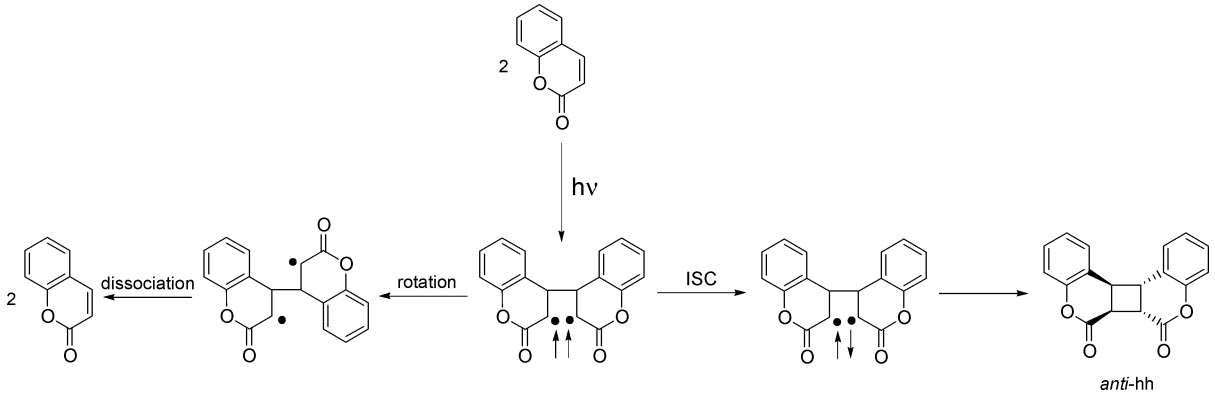

to maintain similar overall composition. For the case of the $Cp'_2Mo_2(CO)_6$ and $Cp'_2Fe_2(CO)_4$ molecules, M−M photolysis is thought to occur from a triplet excited state (Scheme 2), and hence the radical cage pair will be formed in an initial triplet state. If there is a spin barrier, the presence of the heavy atom should enhance the rate of intersystem crossing and result in an increased F_{cP} for the radical cage pairs formed from these molecules. If F_{cP} does not change in the presence of the heavy atom, then it is reasonable to conclude there is no spin barrier to recombination for these species. Note that the spin state of the initially formed [Cp^*TiCl_2, Cp^*] cage pair is not known with certainty but some experimental results suggest a triplet state.[83]

Photochemistry. The photochemistry of $Cp'_2Mo_2(CO)_6$ is relatively straightforward at low-energy irradiation (eq 1), which makes this molecule an excellent radical cage pair precursor for both the pump−probe and steady-state methods. The electronic absorption spectrum has two visible bands; the band with $\lambda_{max} = 390$ nm is attributed to a $\sigma \rightarrow \sigma^*$ transition and the band with $\lambda_{max} = 515$ nm is attributed to a $d\pi \rightarrow \sigma^*$ transition.[84] Irradiation into either absorption band leads to Mo−Mo photolysis.[84] Mo−CO bond dissociation also occurs when the 390 nm band is irradiated, and so to keep the reaction clean, the complex was irradiated at 540 nm. (Note that the steady-state method for determining F_{cP} is independent of side reactions,[85] and consequently, the presence of a Mo−CO bond dissociation process would not affect the accurate determination of F_{cP} values for the radical cage pairs.) The electronic spectrum and low-energy photochemistry of the $Cp'_2Fe_2(CO)_4$ molecule are qualitatively similar to that of $Cp'_2Mo_2(CO)_6$. The complex has two electronic absorption bands at $\lambda_{max} = 410$ and 514 nm attributed to $\sigma \rightarrow \sigma^*$ and $d\pi \rightarrow \sigma^*$ transitions, respectively. Irradiation into either leads to photolysis of the Fe−Fe bond (eq 2).[86,87] As was the case with the $Cp'_2Mo_2(CO)_6$ complex, the irradiation wavelength of 540 nm was chosen to minimize Fe−CO bond dissociation.

$Cp^*_2TiCl_2$ also has a two-band visible spectrum, with the higher energy band ($\lambda = 465$ nm) assigned to a Cl → Ti charge transfer and the lower energy band ($\lambda = 582$ nm) to a Cp^* → Ti charge transfer.[88] Irradiation into the lower energy band proceeds according to eq 3.[88] Our pump−probe investigation of $Cp'_2Fe_2(CO)_4$ revealed that its photochemical reactivity is considerably more complicated than that of $Cp'_2Mo_2(CO)_6$.[89,90] For example, instead of an initial photobleaching event, the transient absorption spectrum for $Cp'_2Fe_2(CO)_4$ showed an initial increase in Δ(Absorbance), suggesting the presence of transient species that absorb at the probing wavelength. Anfinrud et al. directly observed such transients during a nanosecond laser flash photolysis study of the photodissociation of $Cp'_2Fe_2(CO)_4$ (eq 2).[90] Because of the additional complexity introduced by these other reactions, the $Cp'_2Fe_2(CO)_4$ and $Cp^*_2TiCl_2$ were not studied using the pump−probe method.

The Heavy Atoms. A simple calculation (see Supporting Information) suggested that a 2.0 M concentration of the heavy atom probe molecule would on average stastically allow for direct contact between each radical cage pair and at least one heavy atom. To test if this concentration was indeed sufficient to bring about a heavy atom effect, the 2.0 M heavy atom/solvent system was tested on the photodimerization of coumarin, a reaction with a known spin barrier. Under selected conditions, when coumarin is irradiated ($\lambda > 350$ nm) in a heavy atom solvent (e.g., carbon tetrachloride), it photodimerizes to give the anti head-to-head product (eq 4).[82] In contrast, irradiation of coumarin in a nonpolar solvent (e.g., benzene) in the absence of a heavy atom or triplet sensitizer does not lead to dimerization (eq 5).[91,92]

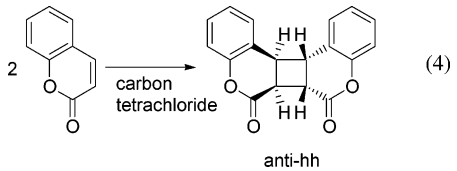

(4)

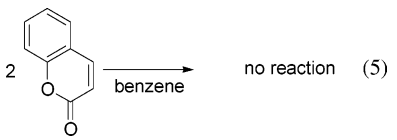

(5)

The accepted explanation for the solvent dependence was proposed by Morrison et al., who suggested that the formation

(83) Endeward, B.; Bernardo, M.; Brant, P.; Thomann, H. *J. Am. Chem. Soc.* **2002**, *124*, 7916−7917.
(84) Wrighton, M. S.; Ginley, D. S. *J. Am. Chem. Soc.* **1975**, *97*, 4246−4251.
(85) Male, J. L.; Lindfors, B. E.; Covert, K. J.; Tyler, D. R. *J. Am. Chem. Soc.* **1998**, *120*, 13176−13186.
(86) Abrahamson, H. B.; Palazzotto, M. C.; Reichel, C. L.; Wrighton, M. S. *J. Am. Chem. Soc.* **1979**, *101*, 4123−4127.
(87) Bergt, M.; Kiefer, B.; Gerber, G. *J. Mol. Struct.* **1999**, *480−481*, 207−210.
(88) Harrigan, R. W.; Hammond, G. S.; Gray, H. B. *J. Organomet. Chem.* **1974**, *81*, 79−85.
(89) Harris, J. D.; Tyler, D. R. Unpublished work.
(90) Anfinrud, P. A.; Han, C. H.; Lian, T.; Hochstrasser, R. M. *J. Phys. Chem.* **1991**, *95*, 574−578.
(91) Hammond, G. S.; Stout, C. A.; Lamola, A. A. *J. Am. Chem. Soc.* **1964**, *86*, 3103−3106.
(92) Schenck, G. O.; Wilucki, I. v.; Krauch, C. H. *Chem. Ber.* **1962**, *95*, 1409−1412.

of dimeric coumarin proceeds through the biradical intermediate shown in Scheme 4.[82]

In this scheme, the intermediate biradical is initially formed in a triplet state. The heavy-atom dependence arises from a competition between rotation of the coumarin halves around the single bond (which is followed by dissociation to reform the coumarin) and ISC of the triplet state to the singlet state (which is followed by formation of the anti head-to-head dimer). When a heavy atom is present, the ISC-dimerization pathway becomes competitive with the rotation-dissociation pathway.[82]

To test that the calculated 2.0 M concentration of heavy atom probe was sufficient to affect the spin barrier, coumarin was irradiated (λ > 350 nm) in neat benzene, in neat carbon tetrachloride, and in solutions of benzene containing either 2.0 M bromobenzene or 2.0 M chlorobenzene. (Iodobenzene was not used because it was found to react photochemically at λ > 350 nm). If the concentration of heavy atom probe is sufficient to facilitate ISC, the formation of anti head-to-head coumarin dimer will result. However, if the concentration is insufficient, then no dimeric product will form. Experiments clearly showed the formation of the anti head-to-head dimeric product in the neat carbon tetrachloride, benzene with 2.0 M bromobenzene, and benzene with 2.0 M chlorobenzene, but not in the neat benzene. (See Supporting Information for details on the identification of the anti head-to-head dimer in these experiments.) From these results, it is concluded that 2.0 M bromobenzene or chlorobenzene in benzene is sufficiently concentrated to cause a heavy atom effect. By extension, 2.0 M iodobenzene is also likely sufficient.[93]

Femtosecond Transient Absorption of $[Cp'Mo(CO)_3]_2$. The dynamics and efficiency of geminate recombination in $Cp'_2Mo_2(CO)_6$ were studied using a two-color femtosecond pump−probe transient absorption experiment with $\lambda_{pump} = 515$ nm and $\lambda_{probe} = 400$ nm. The kinetic transients collected from this experiment are a measurement of the parent dimer population kinetics following the pump-induced photolysis of the Mo−Mo bond. By monitoring the rate and efficiency of the parent bleach recovery following the generation of geminate radical pairs, the hypothesis that an external heavy atom may enhance the recombination rate of the caged pair may be directly investigated. This experimental technique was used earlier to investigate the dynamics of geminate recombination in $Cp'_2Mo_2(CO)_6$.[81] The solvent systems used for the transient absorption studies consisted of a pair of directly comparable solvent compositions that were formulated to be distinguished solely by the presence of an external heavy atom: one solution was *ca.* 1 mM $Cp'_2Mo_2(CO)_6$ and 2.0 M *p*-dichlorobenzene in benzene ($\eta_{solution} = 0.73 \pm 0.02$ cP); the other solution (the control solution) was *ca.* 1 mM $Cp'_2Mo_2(CO)_6$ and *ca.* 0.1 M squalane in benzene ($\eta = 0.73 \pm 0.02$ cP). Exact matching of the solvent viscosities for this pair was achieved through the precise addition of squalane, an inert viscogen, to the control solution. The kinetic traces obtained from the pump−probe spectroscopic analysis of these two solutions are shown below in Figure 1.

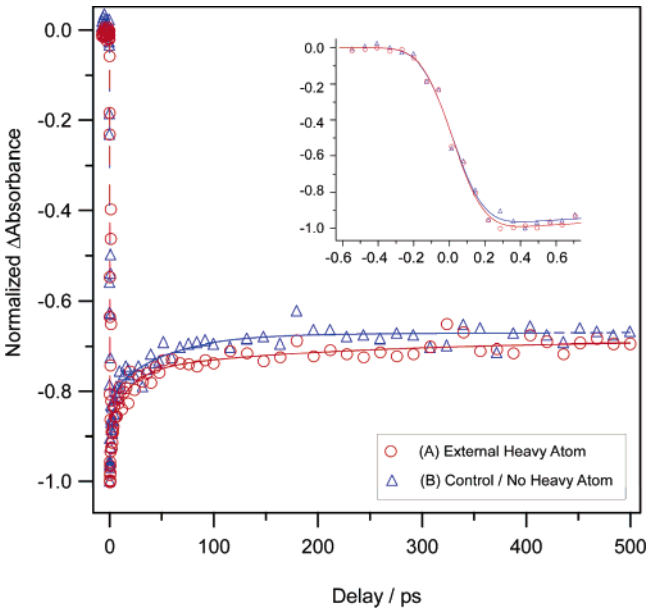

Figure 1. Femtosecond pump−probe transient-absorption kinetic traces of $Cp'_2Mo_2(CO)_6$. The kinetic traces display a transient bleach and partial recovery at $\lambda_{probe} = 400$ nm following photolysis at $\lambda_{pump} = 515$ nm. The inset displays the shortest-time event measured, the instrument-limited Gaussian spike, demonstrating the *ca.* 150 fs resolution of the instrument. The solvent compositions studied are *ca.* 1 mM $Cp'_2Mo_2(CO)_6$/benzene with *p*-dichlorobenzene (○) and the control sample with no external heavy atom (△). The dashed lines represent empirical fits to the data (see text).

The kinetic traces are found to fit satisfactorily to the biexponential function in eq 6,

$$\Delta A = [A_1(1 - \exp(-t/\tau_1)) + A_2(1 - \exp(-t/\tau_2)) + A_3] \times \mathrm{IRF} \quad (6)$$

in which ΔA represents the time-dependent differential absorption, A_1 and A_2 are the pre-exponential factors for the respective exponential rise-to-max functions with time constants τ_1 and τ_2 ($\tau^{-1} = k$), and A_3 is the non-decaying component representing the proportion of un-recovered bleach within the experimental time scale (*ca.* 4 ns). The kinetic equation is convoluted with the instrument response function (IRF) to fit the earliest-time dynamics adequately (eq 7).

$$\mathrm{IRF} = \frac{1}{2}\left[1 + \mathrm{erf}\left(\frac{t - \Delta t}{1.414\sigma}\right)\right] \quad (7)$$

This form is chosen to describe a Gaussian temporal profile with a width parameter, σ, independently determined from a cross-correlation measurement.

The empirically measured kinetics have been interpreted to represent geminate recombination ($\tau_1^{-1} \approx 5$ ps $= k_1^{-1} = k_{cP}^{-1} + k_{dP}^{-1}$) and the subsequent vibrational relaxation of the newly reformed parent dimer ($\tau_2 \approx 100$ ps). On the basis of this model, the cage efficiency factor, F_{cP}, can be extracted from the empirical data fit using the expression in eq 8.

$$F_{cP} = \frac{k_{cP}}{k_{cP} + k_{dP}} = -\frac{A_1 + A_2}{A_3} \quad (8)$$

(93) A reviewer points out that it is conceivable that bromine or other heavy atoms could result in a heavy atom effect in coumarin but not in a transition metal radical cage pair. Specifically, this situation could result if the rate enhancement caused by the heavy atom is comparable to (or faster than) the ISC rate in coumarin but slower than the ISC rate in the transition metal radical cage pair. As shown in the next section, the transition metal cage pairs recombine on the timescale of 5 ps. The timescale of ISC in the transition metal cage pair would thus have to be shorter than 5 ps for this situation to apply. In any case, a radical-radical recombination reaction with a 5 ps timescale would not traditionally be considered to have a spin barrier.

Table 1. Comparison of F_{cP} for the Pump−probe and Steady-state Methods at $\eta = 0.73 \pm 0.02$ cP for $Cp'_2Mo_2(CO)_6$ and $Cp'_2Fe_2(CO)_4$ Both With and Without the Presence of a Heavy Atom Probe

	steady-state results		pump−probe results	
molecule	F_{cP} with heavy atom[a]	F_{cP} without heavy atom	F_{cP} with heavy atom[b]	F_{cP} without heavy atom
$Cp'_2Mo_2(CO)_6$	0.30 ± 0.04	0.32 ± 0.03	0.31 ± 0.01	0.31 ± 0.01
$Cp'_2Fe_2(CO)_4$	0.5 ± 0.1	0.5 ± 0.1		

[a] Iodobenzene. [b] *p*-Dichlorobenzene.

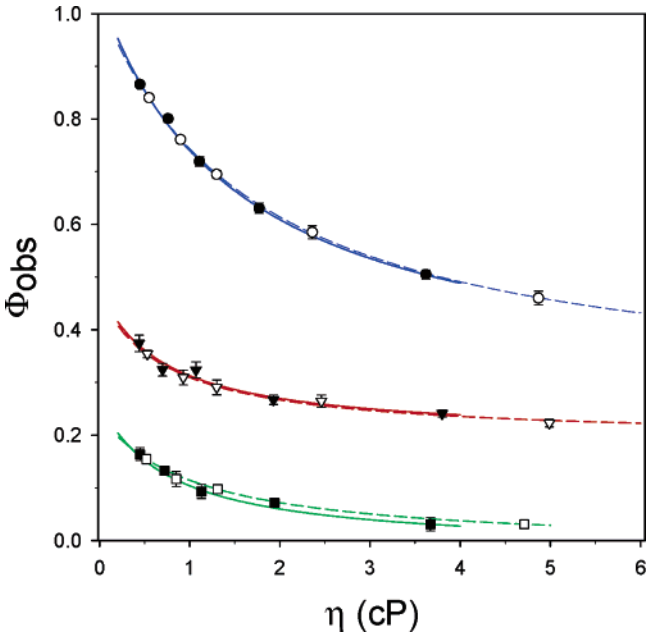

Figure 2. Plot of Φ_{obs} as a function of viscosity for $Cp'_2Mo_2(CO)_6$ (○), $Cp'_2Fe_2(CO)_4$ (▽), and $Cp^*_2TiCl_2$ (□). The filled symbols represent data collected in the presence of 2.0 M chlorobenzene, and the empty symbols represent the data collected in the presence of 2.0 M iodobenzene. The curves are the fits to eq 12; the solid curve is the fit for the data with 2.0 M chlorobenzene, and the dashed curve is the fit for the data with 2.0 M iodobenzene.

A comparison of the F_{cP} values for the two solvent systems is provided in Table 1. Note there is no enhancement of the recombination rate or efficiency with the addition of an external heavy atom. This can be seen qualitatively in the nearly matching kinetic traces in Figure 3.

A potential problem in the interpretation of the results above is that the Cl atoms in the *p*-dichlorobenzene may not be "heavy enough" to act as an external heavy atom, i.e., perhaps ζ_l for Cl is not large enough to overcome the spin barrier by facilitating ISC in the radical cage pair. To address this possibility, the F_{cP} values needed to be obtained using a heavy atom that has a larger ζ_l value, such as Br or I. Unfortunately, a suitable molecule containing bromine or iodine that would not interfere with the pump−probe experiment was not discovered.[94] However, the steady-state method, using iodobenzene as the heavy atom probe, proved to be a suitable resolution to this obstacle. As explained below, this method measures F_{cP} indirectly and requires the use of the trapping agent CCl_4.

(94) The choice of a suitable heavy-atom-containing molecule for use in pump-probe experiments required that the compound be inert toward reaction with the transient radical species, that it not absorb at wavelengths used in the study, and that it has minimal second- and third-order non-linear optical susceptibility coefficients, $\chi^{(2)}$ and $\chi^{(3)}$, to eliminate artifacts that would obscure the results.

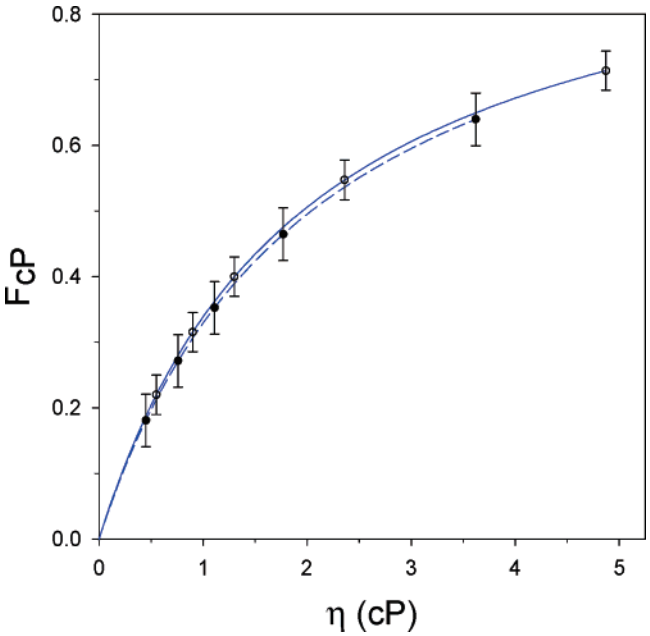

Figure 3. F_{cP} values as a function of viscosity for $Cp'_2Mo_2(CO)_6$. The points represent F_{cP} at measured viscosities. The filled symbols represent data collected in the presence of 2.0 M chlorobenzene, and the empty symbols represent the data collected in the presence of 2.0 M iodobenzene. The curves are the calculated values of F_{cP} obtained using the c parameter obtained from the best fit to eq 12.

Results Using the Steady-State Method. The procedure for obtaining F_{cP} by the steady-state method has been previously described.[95] In brief, the values for F_{cP} were extracted from quantum yield measurements of reactions 9−11 as a function of solvent viscosity. (The solvent viscosity was modified by adding varying amounts of squalane, a viscogen, to the hexanes/CCl_4 solvent.[95])

$$Cp'_2Mo_2(CO)_6 \xrightarrow[\text{hexanes/squalane}]{h\nu\ (546\text{nm})\ CCl_4} 2\ Cp'Mo(CO)_3Cl + [2CCl_3] \quad (9)$$

$$Cp'_2Fe_2(CO)_4 \xrightarrow[\text{hexanes/squalane}]{h\nu\ (546\text{nm})\ CCl_4} 2\ Cp'FE(CO)_2Cl + [2CCl_3] \quad (10)$$

$$Cp^*_2TiCl_2 \xrightarrow[\text{hexanes/squalane}]{h\nu\ (546\text{nm})\ CCl_4} Cp^*TiCl_3 + [Cp^*CCl_3] \quad (11)$$

The quantum yields as a function of viscosity were then fit to eq 12, where c is a fitting parameter that contains k_{cP}, ϕ_{pair} is the quantum yield for formation of the radical cage pair, and ϕ_x is an offset parameter that is necessary to account for a minor electron-transfer reaction that occurs in these systems.[96] The value for F_{cP} was then obtained by inserting the value for ϕ_{pair} into the expression $\Phi_{obs} = \phi_{pair}[1 - F_{cP}]$.

$$\Phi_{obs} = [\phi_{pair}/(1 + \eta/c)] + \phi_x \quad (12)$$

Figure 2 shows the quantum yields for $Cp'_2Mo_2(CO)_6$, $Cp'_2Fe_2(CO)_4$, and $Cp^*_2TiCl_2$ plotted as a function of viscosity. The experiments with and without 2.0 M iodobenzene in solution are shown. Note that the plots are superimposable, which shows the insensitivity of Φ_{obs} to the presence of the external heavy

(95) Schutte, E.; Weakley, T. J. R.; Tyler, D. R. *J. Am. Chem. Soc.* **2003**, *125*, 10319−10326.
(96) Braden, D. A.; Parrack, E. E.; Tyler, D. R. *Photochem. Photobiol. Sci.* **2002**, *1*, 418−420.

atom. As expected based on this superimposability, the F_{cP} vs viscosity plots with and without iodobenzene are likewise superimposable for a particular molecule. Figure 3 shows the F_{cP} values as a function of viscosity for the radical cage pair generated from $Cp'_2Mo_2(CO)_6$. Equally superimposable plots were obtained in the experiments with $Cp'_2Fe_2(CO)_4$, and $Cp^*_2TiCl_2$. In summary, these data strongly suggest there are no spin barriers for recombination of the radical cage pairs [$(CO)_3Cp'Mo\cdot$, $\cdot MoCp'(CO)_3$)], [$(CO)_2Cp'Fe\cdot$, $\cdot FeCp'(CO)_2$], and [$Cl_2Cp^*Ti\cdot$, $\cdot Cp^*$]. A comparison of the F_{cP} values for these solvent data is provided in Table 1.

Summary. Considerable prior work has shown that the spin state of an organic radical cage pair can impact its reactivity. Specifically, because singlet cage pairs can recombine but triplet cage pairs cannot, this can lead to differences in both the descriptive and quantitative aspects of reactivity. No studies to our knowledge have investigated the effect of spin on the reactivity of organometallic radical cage pairs. In this study, the effects of an external heavy atom (present as either iodobenzene or *p*-dichlorobenzene) on the F_{cP} values for radical cage pairs containing Mo ($\zeta_l = 678$ cm^{-1}), Fe ($\zeta_l = 431$ cm^{-1}), and Ti ($\zeta_l = 123$ cm^{-1}) centered radicals were explored. The results (Table 1) showed F_{cP} was insensitive to the presence of the heavy atoms, which suggests there is no spin-barrier to radical−radical recombination. The implication is that ISC is facile for transition metal-centered radical cage pairs (even for first-row transition metals) and that the reactivity of these species is independent of the spin state of the caged radical pair.

Acknowledgment. This work was generously supported by the NSF(CHE-0452004). Dr. Lev Zakharov is acknowledged for his help with obtaining the X-ray crystal structure of the dimeric coumarin molecule.

Supporting Information Available: Discussion of the calculation of the concentration of heavy atom used in these experiments; characterization of the anti-head-to-head coumarin dimer, including crystallographic information and an ORTEP drawing; ^{1}H NMR spectra for the photodimerization of coumarin in neat benzene, neat carbon tetrachloride, 2.0 M chlorobenzene in benzene, and 2.0 M iodobenzene in benzene; UV−vis spectra for the dark reactions between $Cp'_2Mo_2(CO)_6$, $Cp'_2Fe_2(CO)_4$, and $Cp^*_2TiCl_2$ and 2.0 M chlorobenzene in hexane, 2.0 M iodobenzene in hexane, and 2.0 M p-chlorobenzene in benzene; UV−vis spectrum of $Cp'_2Mo_2(CO)_6$, $Cp'_2Fe_2(CO)_4$, and $Cp^*_2TiCl_2$ irradiated for 2 h in hexane with either 2.0 M chlorobenzene or 2.0 M iodobenzene, and for 5 h in benzene with 2.0 M p-dichlorobenzene; four additional references. This material is available free of charge via the Internet at http://pubs.acs.org.

JA069295S